PAPER

CrossMark
click for updates

A one-dimensional coordination polymer based on Cu₃-oximato metallacrowns bridged by benzene-1,4-dicarboxylato ligands: structure and magnetic properties†

Lilia Croitor,*[a] Eduard B. Coropceanu,[b] Oleg Petuhov,[b] Karl W. Krämer,[c] Svetlana G. Baca,[a] Shi-Xia Liu,[c] Silvio Decurtins[c] and Marina S. Fonari[a]

A one-dimensional linear coordination polymer $\{[Cu_3(\mu_3\text{-}OH)(2\text{-}pyao)_3(bdc)]\cdot 6(H_2O)\}_n$ (**1**) composed of trinuclear $[Cu_3(\mu_3\text{-}OH)(2\text{-}pyao)_3]^{2+}$ metallacrown cores bridged by bis-carboxylato linkers has been obtained by treatment of copper(II) fluoride with pyridine-2-aldoxime (2-pyaoH) ligand and benzene-1,4-dicarboxylic acid (H_2bdc). Magnetic susceptibility measurements show strong antiferromagnetic interactions between Cu(II) centers within the trinuclear metallacrown core with $J = -430$ cm^{-1}.

Introduction

Metallacrowns (MCs) are a family of macrocyclic inorganic complexes with structural and functional similarity to crown ethers,[1] that are composed of the $-[M-N-O]_n-$ repeating unit. The interest in the synthesis of copper(II) MC complexes and in the study of their properties is in the current focus due to their involvement in several catalytic processes in living organisms.[2] For example, multicopper blue oxidases contain a triangular unit of copper atoms.[3] In addition, cyclic trinuclear Cu(II) complexes can be regarded as spin-frustrated systems leading to unusual electronic properties[3e,4] and therefore offer the opportunity to test magnetic exchange models which is a very topical issue in the field of molecular magnetism.[4] In recent years, Cu₃-oximato clusters derived from pyridine-2-oximes, (Py)C(R)NOH,[5] have yielded a surprisingly rich chemistry: copper(II) 9-MC-3 have been reported for R = H,[6] CN,[7] Ph[8] or Py.[8a,9] Furthermore, several reports have appeared aiming to increase the nuclearity of magnetic clusters or to link small magnetic clusters through the self-assembly process towards the formation of multidimensional networks.[10] These cores

can further be extended to higher dimensional networks by other organic or inorganic linkers.[10b–d] The connection of Cu₃ units in larger aggregates, *e.g.* their dimerization, has been achieved in a few cases by a μ_4-oxo bridge (Scheme 1a),[11] H-bonds between μ_3-O/μ_3-OH-centered triangles (Scheme 1b),[12] and NO₃⁻, Cl⁻, and ClO₄⁻ anions (Scheme 1c–e),[13,14] as well as *via* additional donor arms or large flexible linkers between oximato groups (Scheme 1f).[8a,12b,13] Notably, only a few examples of coordination polymers built up from the Cu₃ coordination cores have been reported so far, namely 1D *catena*-((μ₃-hydroxo)-tris(μ₂-N-oxy-1-phenyl-1-(pyridin-2-yl)-

[a] *Institute of Applied Physics, Academy of Sciences of R. Moldova, Academy str., 5 MD2028 Chisinau, Moldova. E-mail: croitor.lilia@gmail.com; Fax: +373 22 725887; Tel: +373 22 738154*
[b] *Institute of Chemistry, Academy of Sciences of R. Moldova, Academy str., 3 MD2028 Chisinau, Moldova*
[c] *Department of Chemistry and Biochemistry, University of Bern, Freiestrasse 3, 3012 Bern, Switzerland*
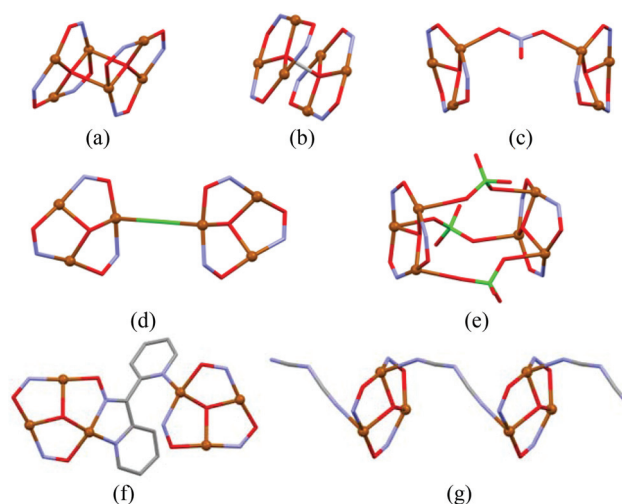
Scheme 1 Selected dimeric and 1D polymeric aggregates of 9-MC-3 Cu(II) units as deposited at CSD through: (a) μ₄-O; (b) μ₃-O/μ₃-OH; (c) NO₃⁻; (d) Cl⁻; (e) ClO₄⁻; (f) 2-pyrazylaldoxime and (g) μ₂-dicyanamide.
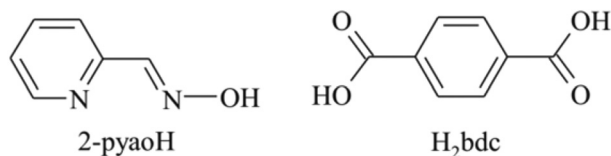
Scheme 2 Schematic illustration of the ligands with acronyms used in this study.

methanimine)-(μ_2-dicyanamide)-(acetato)-tri-copper(II),[8b] 1D *catena*-(bis(μ_3-hydroxo)-bis(μ_3-N-oxy-1-(pyrazin-2-yl)ethanimine)-tetrakis(μ_2-N-oxy-1-(pyrazin-2-yl)ethanimine)-bis(methanol)-bis-(nitrato-O)-hexa-copper dinitrate), and 3D *catena*-(bis(μ_3-N-oxy-1-(pyrazin-2-yl)ethanimine)-(μ_3-oxo)-di-copper bis(tetrafluoro-borate)).[13] In the first one, the linkage of triangular Cu_3 cores occurs through the "innocent" μ_2-dicyanamide, $N(CN)_2^-$ ligand, while in two other structures the extension occurs through pyrazyloximato ligands.

Dicarboxylic acids, aromatic and aliphatic ones, demonstrate their excellent bridging functions in the metal–organic networks.[15] Recently, we have reported some examples of 1D and 2D coordination polymers derived from the Zn/Cd oxime-chemistry, where the [M-pyridine-n-oxime] (n = 2, 4) mononuclear or binuclear units are combined into 1D and 2D polymeric networks *via* bridging benzene-1,4-dicarboxylato, malonato, succinato or adipato linkers.[16] In continuing this research we report here the preparation, structural characterization and magnetic study of a novel 1D coordination polymer, $\{[Cu_3(\mu_3\text{-}OH)(2\text{-}pyao)_3(bdc)]\cdot 6(H_2O)\}_n$ (**1**) (2-pyaoH = pyridine-2-aldoxime, H_2bdc = benzene-1,4-dicarboxylic acid), composed of trinuclear $[Cu_3(\mu_3\text{-}OH)(2\text{-}pyao)_3]^{2+}$ cations bridged by bdc^{2-} linkers (Scheme 2) into chains.

Experimental

Materials and general methods

All reagents and solvents were obtained from commercial sources and were used without further purification. Elemental analysis was performed on an Elementar Analysensysteme GmbH Vario El III elemental analyzer. The IR spectrum was recorded by the ATR-IR spectroscopic technique on a FT IR Spectrum-100 Perkin Elmer spectrometer in the range of 650–4000 cm^{-1}. The UV-Vis absorption spectrum was recorded on a UV-Vis Lambda 25 Perkin Elmer spectrometer. The thermogravimetric analysis (TGA) was carried out with a Derivatograph Q-1500 thermal analyzer in an air flow at a heating rate of 5 °C min^{-1} in the temperature range of 25–1000 °C. The nitrogen adsorption–desorption isotherm has been measured using an Autosorb-1MP device. Magnetic susceptibility data were recorded using a Quantum design MPMS-5XL SQUID magnetometer in the temperature range 1.9–280 K and at a field of 1 kG. Experimental data were corrected for sample holder and diamagnetic contributions ($-0.45 \times$ molecular weight $\times 10^{-6}$ cm^3 mol^{-1}).

Synthesis of $\{[Cu_3(\mu_3\text{-}OH)(2\text{-}pyao)_3(bdc)]\cdot 6(H_2O)\}_n$ (**1**)

CuF_2 (0.01 g, 0.1 mmol) and 2-pyaoH (0.024 g, 0.2 mmol) were dissolved in a mixture of H_2O–CH_3OH–dmf (1 : 3 : 1, 40 ml). The solution was heated and stirred for 10 min, and then H_2bdc (0.017g, 0.1 mmol) was added. The resulting solution was heated for 10 min, filtered off, and then slowly cooled to room temperature giving blue crystals. The crystals were washed with water and air-dried. They are soluble in alcohols, dmf, and partially in water. Yield 73%. Calc. for $C_{52}H_{40}Cu_6N_{12}O_{22}$: C 39.88; H 2.57; N 10.74. Found C 39.31; H 2.14; N 10.48%. IR (cm^{-1}): 3375 (m), 3097 (w), 3037 (w), 1648 (w), 1605 (s), 1562 (s), 1537 (s), 1474 (s), 1442 (m), 1370 (s), 1346 (m), 1301 (w), 1262 (w), 1218 (m), 1117 (vs), 1095 (vs), 1054 (m), 1041 (sh), 886 (m), 810 (m), 774 (sh), 753 (m), 685 (m).

X-ray crystallography

A blue block-shaped crystal with dimensions 0.18 × 0.16 × 0.05 mm was used for structural analysis at 293(2) K on a Xcalibur "Oxford Diffraction" diffractometer equipped with a CCD area detector and a graphite monochromator utilizing Mo Kα radiation. Final unit cell dimensions were obtained and refined on an entire data set. All calculations to solve the structure and to refine the proposed model were carried out with the programs SHELXS97 and SHELXL97.[17] The structure was solved by direct methods and refined by full-matrix least-squares methods on F^2 by using the SHELXL97 program package. All non-hydrogen atoms were refined anisotropically. Hydrogen atoms attached to carbon atoms were placed in geometrically idealized positions and refined by using a riding model. For the disordered solvent water molecules, hydrogen atoms were not localized. The X-ray data and the details of the refinement for **1** are summarized in Table 1. Selected geometric parameters for **1** are given in Table 2. The figures were

Table 1 Crystal and structure refinement data for compound **1**

Empirical formula	$C_{52}H_{40}Cu_6N_{12}O_{22}$
Formula weight	1566.20
Crystal system	Triclinic
Space group	$P\bar{1}$
Z	2
a (Å)	9.9884(11)
b (Å)	17.0223(11)
c (Å)	19.465(2)
α (°)	75.950(8)
β (°)	84.262(9)
γ (°)	80.032(7)
V (Å^3)	3156.3(5)
D_c (g cm^{-3})	1.648
μ (mm^{-1})	2.069
$F(000)$	1572
Crystal size (mm)	0.18 × 0.16 × 0.05
Reflections collected/unique	17882/11335 [R(int) = 0.0504]
Reflections with [$I > 2\sigma(I)$]	6146
Data/restraints/parameters	11335/0/865
GOF on F^2	1.100
R_1, wR_2 [$I > 2\sigma(I)$]	0.0694, 0.0931
R_1, wR_2 (all data)	0.1405, 0.1106

Table 2 Selected bond lengths (Å) and angles (°) in the coordination environment of Cu(II) in **1**

Cu(1)–O(4)	1.962(5)	Cu(4)–O(2)	1.946(4)
Cu(1)–O(1)	1.967(4)	Cu(4)–N(7)	1.976(6)
Cu(1)–N(2)	1.977(6)	Cu(4)–N(8)	1.985(6)
Cu(1)–N(1)	2.008(5)	Cu(4)–O(7)	1.983(5)
Cu(1)–O(10)	2.252(4)	Cu(4)–O(15)	2.267(4)
Cu(2)–O(1)	1.940(4)	Cu(5)–O(8)	1.961(4)
Cu(2)–O(5)	1.968(5)	Cu(5)–O(2)	1.962(5)
Cu(2)–N(4)	1.974(6)	Cu(5)–N(10)	1.996(6)
Cu(2)–N(3)	1.985(6)	Cu(5)–N(9)	1.990(5)
Cu(2)–O(14)	2.306(4)	Cu(5)–O(12)	2.242(4)
Cu(3)–O(3)	1.964(4)	Cu(6)–O(6)	1.970(4)
Cu(3)–O(1)	1.971(4)	Cu(6)–O(2)	1.965(4)
Cu(3)–N(5)	1.988(5)	Cu(6)–N(11)	1.974(6)
Cu(3)–N(6)	2.006(6)	Cu(6)–N(12)	2.008(5)
Cu(3)–O(9)	2.245(4)	Cu(6)–O(11)	2.238(4)
O(4)–Cu(1)–O(1)	93.46(18)	O(2)–Cu(4)–N(7)	88.3(2)
O(4)–Cu(1)–N(2)	170.30(19)	O(2)–Cu(4)–N(8)	168.7(2)
O(1)–Cu(1)–N(2)	88.6(2)	N(7)–Cu(4)–N(8)	81.7(2)
O(4)–Cu(1)–N(1)	94.6(2)	O(2)–Cu(4)–O(7)	94.37(19)
O(1)–Cu(1)–N(1)	164.3(2)	N(7)–Cu(4)–O(7)	159.4(2)
N(2)–Cu(1)–N(1)	81.2(2)	N(8)–Cu(4)–O(7)	93.2(2)
O(4)–Cu(1)–O(10)	89.09(19)	O(2)–Cu(4)–O(15)	94.34(16)
O(1)–Cu(1)–O(10)	89.65(16)	N(7)–Cu(4)–O(15)	105.3(2)
N(2)–Cu(1)–O(10)	100.41(19)	N(8)–Cu(4)–O(15)	93.5(2)
N(1)–Cu(1)–O(10)	103.92(19)	O(7)–Cu(4)–O(15)	94.83(19)
O(1)–Cu(2)–O(5)	94.77(19)	O(8)–Cu(5)–O(2)	92.64(18)
O(1)–Cu(2)–N(4)	168.8(2)	O(8)–Cu(5)–N(10)	95.2(2)
O(5)–Cu(2)–N(4)	93.3(2)	O(2)–Cu(5)–N(10)	163.65(19)
O(1)–Cu(2)–N(3)	89.1(2)	O(8)–Cu(5)–N(9)	173.4(2)
O(5)–Cu(2)–N(3)	159.4(2)	O(2)–Cu(5)–N(9)	89.6(2)
N(4)–Cu(2)–N(3)	80.6(2)	N(10)–Cu(5)–N(9)	81.2(3)
O(1)–Cu(2)–O(14)	91.44(16)	O(8)–Cu(5)–O(12)	98.01(18)
O(5)–Cu(2)–O(14)	92.08(18)	O(2)–Cu(5)–O(12)	97.33(18)
N(4)–Cu(2)–O(14)	95.93(19)	N(10)–Cu(5)–O(12)	95.8(2)
N(3)–Cu(2)–O(14)	108.0(2)	N(9)–Cu(5)–O(12)	87.84(19)
O(3)–Cu(3)–O(1)	93.19(17)	O(6)–Cu(6)–O(2)	93.25(17)
O(3)–Cu(3)–N(5)	176.7(2)	O(6)–Cu(6)–N(11)	171.0(2)
O(1)–Cu(3)–N(5)	88.6(2)	O(2)–Cu(6)–N(11)	88.0(2)
O(3)–Cu(3)–N(6)	96.1(2)	O(6)–Cu(6)–N(12)	95.5(2)
O(1)–Cu(3)–N(6)	163.24(19)	O(2)–Cu(6)–N(12)	162.0(2)
N(5)–Cu(3)–N(6)	81.5(2)	N(11)–Cu(6)–N(12)	81.0(3)
O(3)–Cu(3)–O(9)	92.27(17)	O(6)–Cu(6)–O(11)	87.91(18)
O(1)–Cu(3)–O(9)	99.78(18)	O(2)–Cu(6)–O(11)	92.57(16)
N(5)–Cu(3)–O(9)	90.1(2)	N(11)–Cu(6)–O(11)	101.0(2)
N(6)–Cu(3)–O(9)	93.8(2)	N(12)–Cu(6)–O(11)	103.42(19)

produced using the Mercury program.[18] The solvent accessible voids (SAVs) were calculated using PLATON.[19] CCDC 1047595 contains the supplementary crystallographic data for **1**.

Results and discussion

General

The crystals of compound **1** were obtained by solvent cocrystallization of components in a 1 : 2 : 1 molar ratio of water–methanol–dmf solution. The dark blue crystals with an irregular shape are air-stable (Fig. 1S in ESI†). The optical absorption spectrum recorded in methanol solution reveals two bands (Fig. 2S†). The strongest band appears at λ_{max} = 240 nm, which is predominantly due to an intraligand charge transfer (ILCT),

and another one at λ_{max} = 332 nm is due to a ligand to ligand charge transfer (LLCT). The IR spectrum of compound **1** shown in Fig. 3S† confirms the presence of the organic ligands through the typical vibrations of benzene/pyridine aromatic rings, oxime and carboxylic groups.[8c] A broad band centered at 3375 cm^{-1} is due to the presence of water molecules. Bands characteristic for the 2-pyao ligand are at 1605 cm^{-1} (s, pyridyl C=N), 1474 cm^{-1} (s, N–O). A strong doublet band (1562 and 1534 cm^{-1}) is attributed to $\nu_{asym}(CO_2)$, and a strong doublet band (1370 and 1346 cm^{-1}) is attributed to $\nu_{sym}(CO_2)$. Vibrational peaks in the region 810–680 cm^{-1} are assigned to C–H deformation modes.

Crystallography

Compound **1** crystallizes in the triclinic space group $P\bar{1}$. The asymmetric unit comprises two similar triangular $[Cu_3(\mu_3\text{-}OH)(2\text{-}pyao)_3]$ cores bonded through two crystallographically different bdc^{2-} ligands (Fig. 1a). The geometry around each of the copper(II) ions in the trimeric unit is best described as a distorted square pyramid having a N$_2$O$_3$ coordination environment. The degree of distortion for five-coordinated complexes is indicated by the general descriptor $\tau = (\beta - \alpha)/60$,[20] where α and β are the two largest angles at the metal center. For the idealized square pyramidal extreme $\tau = 0$. In compound **1** τ values are in the range of 0.1–0.225. The trimeric skeletons are created by the pyridine N atom and the oximato nitrogen and oxygen atoms of three 2-pyao ligands, while the O atom of the μ_3-OH ligand [O(1), O(2)] completes the square-planar bases of the three metal atoms, with Cu–O bond distances in the range of 1.940(4)–1.971(4) Å. The Cu$_3$ triangles and the bdc^{2-} ligands are assembled to form a one-dimensional polymer where two bdc^{2-} molecules bridge the Cu(1,2,3) and Cu(4,5,6) units with alternating mono- and bidentate bridging modes (Fig. 1b). The slight asymmetry in each triangle is derived from this different bdc^{2-} coordination on opposite sides of the trimeric units. Thereby, one coordinates in a bis-bidentate and another in a bis-monodentate mode while linking to different Cu(II) atoms. A similar asymmetry was also observed for other carboxylates with 2,4,5-trichlorophenoxy,[8c] acetato,[13] benzoato,[9,13] and perchlorato[11a] and nitrato[21] ligands. The bis-bidentate bdc^{2-} ligand bridges Cu(1) and Cu(3) [Cu(1)–O(10) = 2.252(4) Å, Cu(3)–O(9) = 2.245(4) Å], and Cu(5) and Cu(6) [Cu(5)–O(12) = 2.242(4) Å, Cu(6)–O(11) = 2.238(4) Å]. It alternates in the polymeric chain with the bis-monodentate ligand which bridges Cu(2) and Cu(4) [Cu(2)–O(14) = 2.306(4) Å and Cu(4)–O(15) = 2.267(4) Å]. All these oxygen atoms occupy the apical positions of the distorted square-base pyramids. In addition, hydrogen bonds are formed from the bis-monodentate ligand to the μ_3-OH ligand of the metallacrown ring with O(1)–H(1)···O(13) = 1.67 Å [O···O = 2.604(5) Å] and O(2)–H(2)···O(16) = 1.67 Å [O···O = 2.591(5) Å]. The torsion angles between the Cu(II) ions across the oximato-bridges are −22.96° for Cu(1)–O(4)–N(3)–Cu(2), 5.59° for Cu(2)–O(5)–N(5)–Cu(3), −14.52° for Cu(3)–O(3)–N(2)–Cu(1), −3.04° for Cu(4)–O(7)–N(9)–Cu(5), 10.92° for Cu(5)–O(8)–N(11)–Cu(6), and 24.92° for Cu(6)–O(6)–N(7)–Cu(4). The central μ_3-OH ligands are placed 0.603 and 0.613 Å
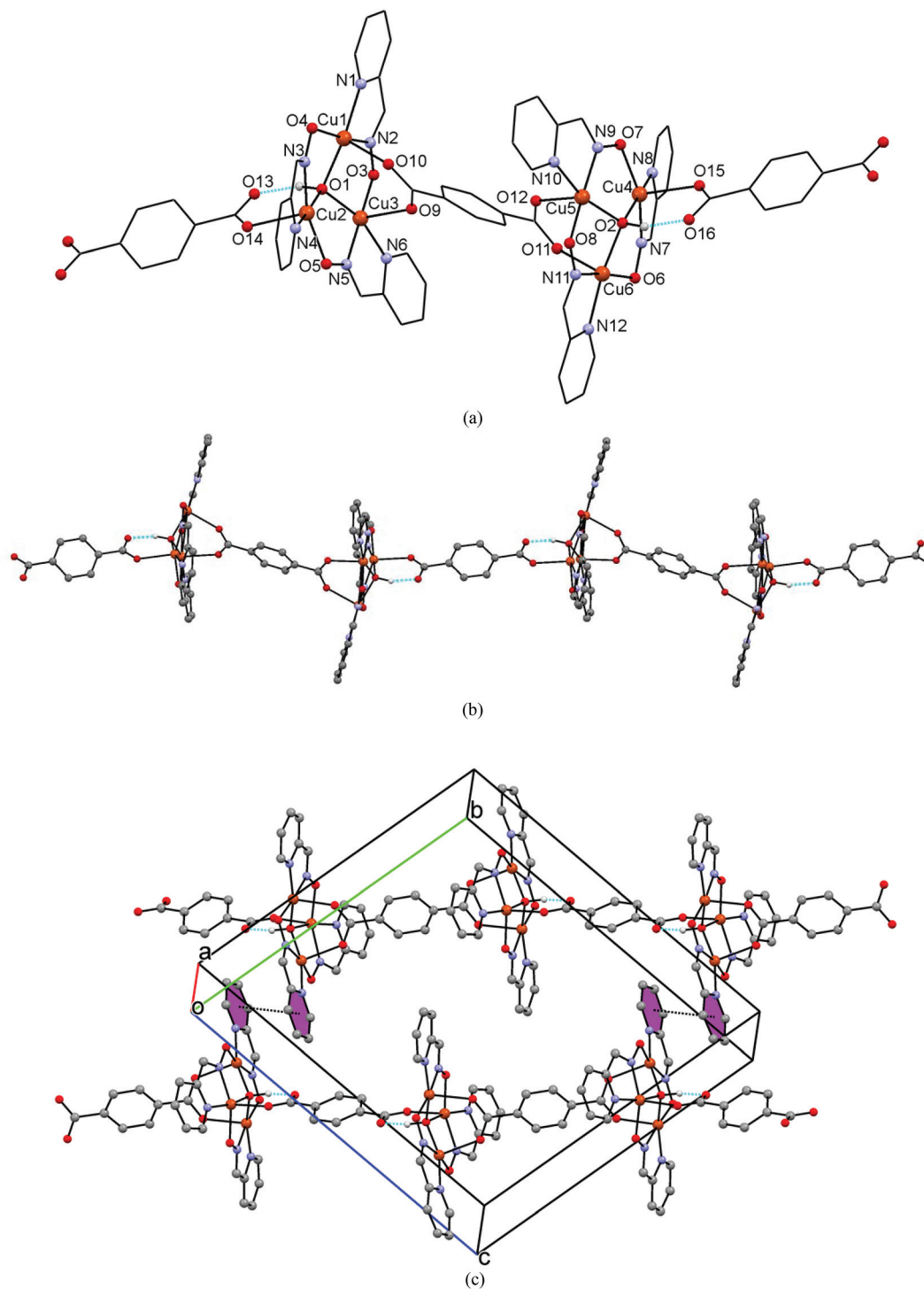
(a)

(b)

(c)

Fig. 1 Molecular and crystal structure of **1**. (a) Two crystallographically different Cu_3 cores separated by a bdc^{2-} ligand with partial numbering scheme. (b) Fragment of a 1D polymeric chain showing the concave shapes of Cu_3 cores. (c) Packing of 1D chains sustained by $\pi-\pi$ stacking interactions between the partially overlapping pyridine rings. The centroid···centroid distance between the colored rings is 3.671 Å.

above the Cu(1,2,3) and Cu(4,5,6) planes, respectively. The Cu_3 units form scalene triangles, however they are close to equilateral triangles with Cu(1)···Cu(2), Cu(2)···Cu(3), Cu(1)···Cu(3) distances of 3.229, 3.279, and 3.154 Å, and Cu(4)···Cu(5), Cu(5) ···Cu(6), and Cu(4)···Cu(6) distances of 3.267, 3.154 and 3.255 Å, respectively. The Cu_3 triangles are situated in approximately parallel planes as the interplanar angle of 3.11° between the Cu_3 cores indicates. The shortest Cu···Cu separ-

ations across the bis-bidentate bridging bdc^{2-} ligand are 11.296 and 11.350 Å, while across the bis-monodentate bridging ligand it is 11.830 Å.

The structure of the 1D polymer **1** was refined as a hydrate with the overall uptake of six disordered water molecules per formula unit. The molecular packing was analyzed by the Mercury program.[18] It indicates negligible solvent accessible voids (SAVs) for the hydrated structure (2.3% of the unit cell volume calculated with the accommodated water molecules). The SAVs for the solvent-free network give a value of 531.4 Å^3 (~16.8% of the unit cell volume), thus indicating the high solvent uptake. The packing of the coordination polymers reveals π-stacking interactions between a pair of inversion-related 2-pyao pyridine rings (Fig. 1c). One might speculate that a similar stacking between the next pairs of 2-pyao-rings is precluded by the water accommodation in the crystal lattice situated in the hydrophilic regions in proximity to the carboxylic groups (Fig. 4S†).

Thermal stability and sorption properties

To estimate the thermal stability of **1**, a thermogravimetric analysis (TGA) was undertaken. The TGA plots indicate at least a four-stage decomposition process in an air atmosphere (Fig. 5S†). In the temperature range of 25–160 °C, two maxima are observed and assigned to the solvent water loss. This gradual loss corresponds to the removal of four water molecules in the temperature range of 25–105 °C (8.40%), and two water molecules in the range of 105–160 °C (4.05%). This stepwise process is explained by the different modes of water association in the crystal, in line with the reported data for the hydrated mixed-ligand Cu(II) terephthalates.[22] The sample mass decreases by 12.45% (calculated 12.80%). The dehydrated sample remains stable in the temperature range of 160–236 °C. At 236 °C a rapid decomposition of the compound starts, resulting in a loss of 48.8% by weight. The decomposition is accompanied by a strong exothermic effect. Although decarboxylation and CO removal is the most favorable process for this stage,[22] the significant weight loss indicates that fragmentation is not so simple and that decomposition steps are strongly overlapped and include also the degradation of the Cu$_3$ core.[23] The final thermal degradation with a loss of 11.06% mass is also accompanied by an exothermic heat effect. From 354 °C on, the degradation product (possibly copper(II) oxide) is stable up to 1100 °C. The total loss is 73.20% (calculated 71.56%).

The N$_2$ sorption isotherm was recorded for the dehydrated **1** (Fig. 6S†). The compound hardly adsorbs N$_2$ at 77 K, which leads to the insignificant BET (Brunauer–Emmett–Teller) surface area of 9.9 m^2 g^{-1}. Near saturation pressure, there is a sudden increase in sorption caused by condensation of nitrogen; this can be explained by the presence of mesopores. The total pore volume constitutes 0.046 cm^3 g^{-1}. As it is evidenced from Fig. 6S,† the hysteresis loop is caused by these mesopores.

Magnetic properties and structure–property correlation

Compound **1** was studied by magnetic susceptibility measurements. The $\chi_m T(T)$ plot (Fig. 2) of a polycrystalline sample of **1** shows a room temperature value of 0.47 cm^3 K mol^{-1} per Cu$_3$ which is much lower than that expected for three uncoupled spins with $S = 1/2$; this is an evidence for strong antiferromagnetic coupling. Upon cooling, the $\chi_m T$ values reach a declining plateau of about 0.4 cm^3 K mol^{-1} until they decrease again at temperatures below 80 K to reach 0.26 cm^3 K mol^{-1} at 1.9 K. At the plateau, the $\chi_m T$ values of about 0.4 cm^3 K mol^{-1} correspond to those of an isolated $S = 1/2$ ground state with an usual g value for Cu(II). A strikingly similar behavior was observed for triangular μ_3-OH/oximato Cu(II)$_3$ complexes in a recent study by Escuer et al.[14a] The magnetization data taken at 1.9 K confirm the $S = 1/2$ ground state of the Cu$_3$ unit (see Fig. 7S†).

It is well known that for an equilateral triangular Cu(II)$_3$ complex, the isotropic exchange interaction yields two degenerate spin doublets (^{2}E) as the ground state, separated from a spin quadruplet (^{4}A) state through an energy gap of 3J/2. This result is directly deduced from the isotropic exchange Hamiltonian: $H_{iso} = -J_{12}S_1 \cdot S_2 - J_{13}S_1 \cdot S_3 - J_{23}S_2 \cdot S_3$, with $J_{12} = J_{13} = J_{23} = J$ for the equilateral case.

Approximating a trinuclear system with an isosceles triangle (thus, the closer Cu(II) ions are treated as equivalent) gives $J = J_{12} = J_{23} \neq J_{13} = j$ and $\delta = J - j$. At this level of theory, the high temperature behavior including the temperature region representing the plateau of the $\chi_m T$ values can be analyzed. However, following the discussions in the work of Escuer et al.[14a] and Ferrer et al.,[14b] the magnetic behavior at low temperatures is attributed to antisymmetric exchange (ASE) interactions within the trimeric units. The corresponding Hamiltonian is described by

$$H_{ASE} = G_{12}[S_1 \times S_2] + G_{23}[S_2 \times S_3] + G_{31}[S_3 \times S_1]$$

where $[S_i \times S_j]$ and G_{ij} are the vector product and the antisymmetric vector ($G_{ij} = -G_{ji}$), respectively. On the basis of an axial
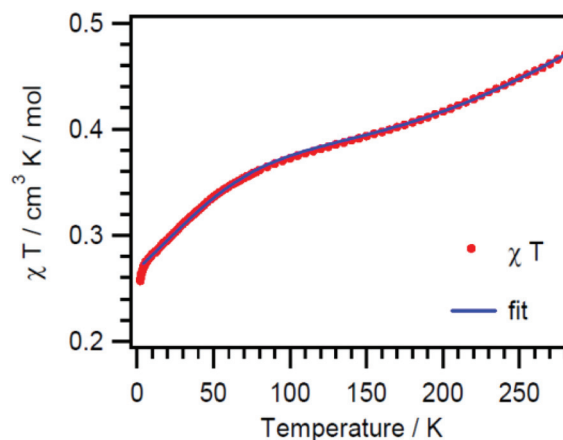

Fig. 2 Thermal variation of $\chi_m T$ for **1** per Cu$_3$ (solid line is a fit).

Table 3 Comparison of structural and magnetic parameters concerning the μ_3-OH in Cu_3-oximato clusters[a]

Compound	Topology	O(H) distance from the Cu$_3$ plane/Å	Cu–O(H)/Å (av)	Cu–Cu'/Å (av)	$-J$/cm^{-1}	Reference
1	1D	0.612/0.622	1.961	3.220/3.226	430	Present work
BAQXUO	1D	0.616	1.957	3.215	460	8b
IMIXAE	1D	0.649/0.599	1.967/1.954	3.215/3.221	447	13
IMIXIM	3D	0.393	1.887	3.196	298	13
OXMCUB	0D	0.695	1.964	3.194	122	11b
HOHQUR	0D	0.66	1.942	3.166	220	8c
ILEGEM	0D	0.549	1.934	3.212	411	8f
RIQPOY	0D	0.521	1.972	3.289	615	14
RIQQIT	0D	0.545/0.576	1.982/1.992	3.300/3.303	621	14
RIQQOZ	0D	0.588/0.587	1.972/1.979	3.258/3.268	683	14

[a] BAQXUO = *catena*-((μ$_3$-hydroxo)-tris(μ$_2$-N-oxy-1-phenyl-1-(pyridin-2-yl) methanimine)-(μ$_2$-dicyanamide)-(acetato)-tri-copper(II)); IMIXAE = *catena*-(bis(μ$_3$-hydroxo)-bis(μ$_3$-N-oxy-1-(pyrazin-2-yl)ethanimine)-tetrakis(μ$_2$-N-oxy-1-(pyrazin-2-yl)ethanimine)-bis(methanol)-bis(nitrato-O)-hexa-copper dinitrate); IMIXIM = *catena*-(bis(μ$_3$-N-oxy-1-(pyrazin-2-yl)ethanimine)-(μ$_3$-oxo)-di-copper bis(tetrafluoro-borate)); OXMCUB = bis((μ$_4$-oxo)-tris(μ$_2$-1,2-diphenyl-2-(methylimino)-1-ethanone-oximato-N,N',O)-tri-copper(II)) diperchlorate; HOHQUR = (μ$_3$-hydroxo)-tris(μ$_2$-N-oxy-1,1-diphenylmethanimine-N,N',O)-(μ$_2$-(2,4,5-trichlorophenoxy)acetato-O,O')-((2,4,5-trichloro-phenoxy)acetato-O)-tri-copper(II) methanol solvate; ILEGEM = (μ$_3$-hydroxo)-tris(μ$_2$-phenyl(pyridin-2-yl)methanone oximato-N,N',O)-(methanol-O)-(nitrato-O)-tri-copper(II) nitrate; RIQPOY = (μ$_3$-hydroxo)-(μ$_2$-benzoato-O,O')-tris(μ$_2$-6-methyl-2-pyridylaldoximato)-(benzoato-O)-tri-copper; RIQQIT = bis(μ$_3$-hydroxo)-hexakis(μ$_2$-([(6-methylpyridin-2-yl)methylidene]amino)oxidanide)-tris(μ$_2$-perchlorato)-hexa-copper perchlorate; RIQQOZ = bis(μ$_3$-hydroxo)-hexakis(μ$_2$-([(6-methylpyridin-2-yl)methylidene]amino)oxidanide)-tris(μ$_2$-nitrato)-hexa-copper(II) nitrate monohydrate.

ASE (the justification of it is discussed by Ferrer *et al.*[14b]), the Hamiltonian is reduced to $H_{ASE} = G_Z[S_1 \times S_2 + S_2 \times S_3 + S_3 \times S_1]$. Diagonalization of the total Hamiltonian comprising H_{iso} + H_{ASE} + H_{Zeem} (H_{Zeem} = axial Hamiltonian for the Zeeman interaction) leads to a distinct pattern of energy levels from which the corresponding van Vleck expression can be derived (eqn (4) in ref. 14a). The best-fit values for the experimental $\chi_m T$ values were $J = -430$ cm^{-1}, $j = -338$ cm^{-1}, $G_Z = 60$ cm^{-1}, $g_\parallel = 2.23$, $g_\perp = 2.0$. The theoretical curve calculated from these parameters is shown in Fig. 2. There is no intertrimer interaction included in the analysis. On the one side, it would lead to overparameterization and on the other side (*vide infra*), any such interaction could be expected to be very weak. The resulting best-fit magnetic parameters compare well with literature values.[14a]

A magnetostructural correlation can be discussed based on the actual structural data and the literature data. Table 3 summarizes geometric parameters and J values for the complexes containing a Cu_3-oximato coordination core. It is evident, that geometric parameters such as $Cu\cdots Cu$ and $Cu\cdots\mu_3$-OH distances alter in narrow intervals, while the μ_3-OH distance from the Cu_3 plane varies in the range of 0.393–0.695 Å. The reported 0D complexes reveal higher J values than polymeric ones. Among the polymeric materials the J value is not significantly influenced by the inter-core interaction since it is rather weak, as Chakraborty *et al.* have estimated it.[8b]

Conclusions

In conclusion, the first example of a coordination polymer comprising Cu_3-metallacrowns and 1,4-benzenedicarboxylate bridges is reported. The simple and direct synthetic route employing oxime and dicarboxylate ligands provides a direct access to the polymeric materials composed of paramagnetic Cu_3 units representing spin-frustrated metallacrowns.

Acknowledgements

Notes and references

1 (a) G. Mezei, C. M. Zaleski and V. L. Pecoraro, *Chem. Rev.*, 2007, **107**, 4933–5003; (b) E. Zangrando, M. Casanova and E. Alessio, *Chem. Rev.*, 2008, **108**, 4979–5013.

2 (a) E. I. Solomon, U. M. Sundaram and T. E. Machonkin, *Chem. Rev.*, 1996, **96**, 2563–2606; (b) R. H. Holm, P. Kennepohl and E. I. Solomon, *Chem. Rev.*, 1996, **96**, 2239–2314; (c) W. Kaim and J. Rall, *Angew. Chem., Int. Ed. Engl.*, 1996, **35**, 43–60.

3 (a) N. Kitajima and Y. Moro-oka, *Chem. Rev.*, 1994, **94**, 737–757; (b) E. I. Solomon, F. Tuczek, D. E. Root and C. A. Brow, *Chem. Rev.*, 1994, **94**, 827–856; (c) Y.-B. Jiang, H.-Z. Kou, R.-J. Wang, A.-L. Cui and J. Ribas, *Inorg. Chem.*, 2005, **44**, 709–715; (d) T. C. Stamatatos, J. C. Vlahopoulou, Y. Sanakis, C. P. Raptopoulou, V. Psycharis, A. K. Boudalis and S. P. Perlepes, *Inorg. Chem. Commun.*, 2006, **9**, 814–818; (e) J. Yoon, L. M. Mirica, T. D. P. Stack and E. I. Solomon, *J. Am. Chem. Soc.*, 2005, **127**, 13680–13693; (f) A. Messerschmidt, *Struct. Bonding*, 1998, **90**, 37–68.

4 (a) L. Gutierrez, G. Alzuet, J. A. Real, J. Cano, J. Borras and A. Castineiras, *Inorg. Chem.*, 2000, **39**, 3608–3614; (b) O. Kahn, *Chem. Phys. Lett.*, 1997, **265**, 109–114; (c) S. Ferrer, J. G. Haasnoot, J. Reedijk, E. Muller,

M. B. Cingi, M. Lanfranchi, A. M. M. Lanfredi and J. Ribas, *Inorg. Chem.*, 2000, **39**, 1859–1867; (*d*) X. Liu, M. P. de Miranda, E. J. L. McInnes, C. A. Kilner and M. A. Halcrow, *Dalton Trans.*, 2004, 59–64; (*e*) L. M. Mirica and T. D. P. Stack, *Inorg. Chem.*, 2005, **44**, 2131–2133; (*f*) J. Yoon and E. I. Solomon, *Coord. Chem. Rev.*, 2007, **251**, 379–400; (*g*) G. Pascu, C. Deville, S. E. Clifford, L. Guenée, C. Besnard, K. W. Krämer, S.-X. Liu, S. Decurtins, F. Tuna, E. J. L. McInnes, R. E. P. Winpenny and A. F. Williams, *Dalton Trans.*, 2014, **43**, 656–662; (*h*) A. S. Degtyarenko, M. Handke, K. W. Krämer, S.-X. Liu, S. Decurtins, E. B. Rusanov, L. K. Thompson, H. Krautscheid and K. V. Domasevitch, *Dalton Trans.*, 2014, **43**, 8530–8542; (*i*) O. Kahn, *Molecular Magnetism*, VCH, Weinheim, Germany, 1993; (*j*) M. Pilkington and S. Decurtins, *Chimia*, 2000, **54**, 593–601; (*k*) In Magnetism – Molecular *and Supramolecular Perspectives*, *Coord. Chem. Rev.*, ed. L. K. Thompson, 2005, **249**, 2549–2730.

5 (*a*) P. Chaudhuri, *Coord. Chem. Rev.*, 2003, **243**, 143–190; (*b*) C. J. Milios, T. C. Stamatatos and S. P. Perlepes, *Polyhedron*, 2006, **25**, 134–194.

6 (*a*) R. Beckett and B. F. Hoskins, *J. Chem. Soc., Dalton Trans.*, 1972, 291–295.

7 A. Escuer, G. Vlahopoulou, S. P. Perlepes and F. A. Mautner, *Inorg. Chem.*, 2011, **50**, 2468–2478.

8 (*a*) T. Afrati, C. M. Zaleski, C. Dendrinou-Samara, G. Mezei, J. W. Kampf, V. L. Pecoraro and D. P. Kessissoglou, *Dalton Trans.*, 2007, 2658–2668; (*b*) A. Chakraborty, K. L. Gurunatha, A. Muthulakshmi, S. Dutta, S. K. Pati and T. K. Maji, *Dalton Trans.*, 2012, **41**, 5879–5888; (*c*) T. Afrati, C. Dendrinou-Samara, C. Raptopoulou, A. Terzis, V. Tangoulis, A. Tsipis and D. P. Kessissoglou, *Inorg. Chem.*, 2008, **47**, 7545–7555; (*d*) G.-X. Liu, H.-M. Xu and X.-M. Ren, *Chin. J. Struct. Chem.*, 2010, **29**, 1072–1076; (*e*) T. Afrati, A. A. Pantazaki, C. Dendrinou-Samara, C. Raptopoulou, A. Terzis and D. P. Kessissoglou, *Dalton Trans.*, 2010, **39**, 765–775; (*f*) G.-X. Liu, W. Guo, S. Nishihara and X.-M. Ren, *Inorg. Chim. Acta*, 2011, **368**, 165–169.

9 T. C. Stamatatos, J. C. Vlahopoulou, Y. Sanakis, C. P. Raptopoulou, V. Psycharis, A. K. Boudalis and S. P. Perlepes, *Inorg. Chem. Commun.*, 2006, **9**, 814–818.

10 (*a*) E. E. Moushi, T. C. Stamatatos, W. Wernsdorfer, V. Nastopoulos, G. Christou and A. J. Tasiopoulos, *Angew. Chem., Int. Ed.*, 2006, **45**, 7722–7725; (*b*) W. Quellette, M. H. Yu, C. J. O'Connor, D. Hagrman and J. Zubieta, *Angew. Chem., Int. Ed.*, 2006, **45**, 3497–3500; (*c*) B. Ding, L. Yi, P. Cheng, D. Z. Liao and S. P. Yan, *Inorg. Chem.*, 2006, **45**, 5799–5803; (*d*) M. Casarin, C. Corvaja, C. Di Nicola, D. Falcomer, L. Franco, M. Monari, L. Pandolfo, C. Pettinari, F. Piccinelli and P. Tagliatesta, *Inorg. Chem.*, 2004, **43**, 5865–5876; (*e*) Y. Z. Zheng, M. L. Tong, W. Xue, W. Zhang, X. M. Chen, F. Grandjean and G. J. Long, *Angew.*

Chem., Int. Ed., 2007, **46**, 6076–6080; (*f*) P. Albores and E. Rentschler, *Inorg. Chem.*, 2008, **47**, 7960–7962.

11 (*a*) Y. Agnus, R. Louis, B. Metz, C. Boudon, J. P. Gisselbrecht and M. Gross, *Inorg. Chem.*, 1991, **30**, 3155–3161; (*b*) R. J. Butcher, C. J. O'Connor and E. Sinn, *Inorg. Chem.*, 1981, **20**, 537–545.

12 (*a*) D. Maity, P. Mukherjee, A. Ghosh, M. G. B. Drew, C. Diaz and G. Mukhopadhyay, *Eur. J. Inorg. Chem.*, 2010, 807–813; (*b*) S. Karmakar, O. Das, S. Ghosh, E. Zangrando, M. Johann, E. Rentschler, T. Weyhermuller, S. Khanra and T. K. Paine, *Dalton Trans.*, 2010, **39**, 10920–10927; (*c*) L. K. Das, M. G. B. Drew, C. Diaz and A. Ghosh, *Dalton Trans.*, 2014, **43**, 7589–7598.

13 A. Escuer, B. Cordero, M. Font-Bardia and T. Calvet, *Inorg. Chem.*, 2010, **49**, 9752–9754.

14 (*a*) A. Escuer, G. Vlahopoulou, F. Lloret and F. A. Mautner, *Eur. J. Inorg. Chem.*, 2014, 83–92; (*b*) S. Ferrer, F. Lloret, E. Pardo, J. M. Clemente-Juan, M. Liu-Gonzalez and S. Garcia-Granda, *Inorg. Chem.*, 2012, **51**, 985–1001.

15 (*a*) Y.-Z. Zheng, Z. Zheng and X.-M. Chen, *Coord. Chem. Rev.*, 2014, **258–259**, 1–15; (*b*) B. Dey, A. Das, S. R. Choudhury, A. D. Jana, L.-P. Lu, M.-L. Zhu and S. Mukhopadhyay, *Inorg. Chim. Acta*, 2010, **363**, 981–987; (*c*) X. Xu, Y. Ma and E. Wang, *J. Solid State Chem.*, 2007, **180**, 3136–3145; (*d*) R. A. Sarmiento-Perez, L. M. Rodriguez-Albelo, A. Gomez, M. Autie-Perez, D. W. Lewis and A. R. Ruiz-Salvador, *Microporous Mesoporous Mater.*, 2012, **163**, 186–191.

16 (*a*) L. Croitor, E. B. Coropceanu, A. V. Siminel, A. E. Masunov and M. S. Fonari, *Polyhedron*, 2013, **60**, 140–150; (*b*) L. Croitor, E. B. Coropceanu, A. E. Masunov, H. J. Rivera-Jacquez, A. V. Siminel, V. I. Zelentsov, T. Ya. Datsko and M. S. Fonari, *Cryst. Growth Des.*, 2014, **14**, 3935–3948.

17 G. M. Sheldrick, *Acta Crystallogr., Sect. A: Fundam. Crystallogr.*, 2008, **64**, 112–122.

18 C. F. Macrae, P. R. Edgington, P. McCabe, E. Pidcock, G. P. Shields, R. Taylor, M. Towler and J. van de Streek, *J. Appl. Crystallogr.*, 2006, **39**, 453–457.

19 A. L. Spek, *J. Appl. Crystallogr.*, 2003, **36**, 7–13.

20 (*a*) A. W. Addison, T. N. Rao, J. Reedijk, J. van Rijn and G. C. Verschoor, *J. Chem. Soc., Dalton Trans.*, 1984, 1349–1356; (*b*) E. Melnic, E. B. Coropceanu, O. V. Kulikova, A. V. Siminel, D. Anderson, H. J. Rivera-Jacquez, A. E. Masunov, M. S. Fonari and V. Ch. Kravtsov, *J. Phys. Chem. C*, 2014, **118**, 30087–30100.

21 B. Cordero, A. Escuer, M. Font-Bardia and T. Calvet, *Polyhedron*, 2013, **64**, 84–90.

22 J. Rogan and D. Poleti, *Thermochim. Acta*, 2004, **413**, 227–234.

23 R. Bucci, V. Carunchio, A. D. Magri and A. L. Magri, *J. Therm. Anal.*, 1984, **29**, 679–686.